applied sciences

MDPI

Article

Influence of Seal Cavity Leakage Flow on Compressor Performance Investigated with a Circumferentially Averaged Method

Dong Liang [1], Xingmin Gui [1,2] and Donghai Jin [1,2,*]

[1] School of Energy and Power Engineering, Beihang University, Beijing 100191, China; liangdong5790@buaa.edu.cn (D.L.); guixm@buaa.edu.cn (X.G.)
[2] Jiangxi Research Institute, Beihang University, Nanchang 330096, China
* Correspondence: jdh@buaa.edu.cn; Tel.: +86-01082316870

Featured Application: This method can be used to quickly analyze the performance degradation caused by labyrinth wear in axial compressors. After being verified in multistage compressors and turbine in the future, it can be further used to consider the influence of seal cavity leakage flow in aeroengine simulation.

Abstract: In order to investigate the effect of seal cavity leakage flow on a compressor's performance and the interaction mechanism between the leakage flow and the main flow, a one-stage compressor with a cavity under the shrouded stator was numerically simulated using an inhouse circumferentially averaged through flow program. The leakage flow from the shrouded stator cavity was calculated simultaneously with main flow in an integrated manner. The results indicate that the seal cavity leakage flow has a significant impact on the overall performance of the compressor. For a leakage of 0.2% of incoming flow, the decrease in the total pressure ratio was 2% and the reduction of efficiency was 1.9 points. Spanwise distribution of the flow field variables of the shrouded stator shows that the leakage flow leads to an increased flow blockage near the hub, resulting in drop of stator performance, as well as a certain destructive effect on the flow field of the main passage.

Keywords: seal cavity leakage flow; shrouded stator; flow field destruction; performance drop; circumferentially averaged throughflow model

Citation: Liang, D.; Gui, X.; Jin, D. Influence of Seal Cavity Leakage Flow on Compressor Performance Investigated with a Circumferentially Averaged Method. *Appl. Sci.* **2021**, *11*, 780. https://doi.org/10.3390/app11020780

Received: 1 December 2020
Accepted: 7 January 2021
Published: 15 January 2021

1. Introduction

The seal cavity leakage flow can also be called the 'shrouded stator cavity flow', or 'stator shroud leakage' in compressors, and 'shroud leakage' or 'shroud leakage flow' in turbines. As in Figure 1, in an axial flow compressor or a turbine with a shrouded stator, there is an axial gap between the stationary inner band and the rotating rotor wheel. Although the flow exchange between the main channel and the cavity below the axial gap is often suppressed by engineering measures such as a labyrinth seal, it is difficult to fully eliminate the leakage from the axial gap.

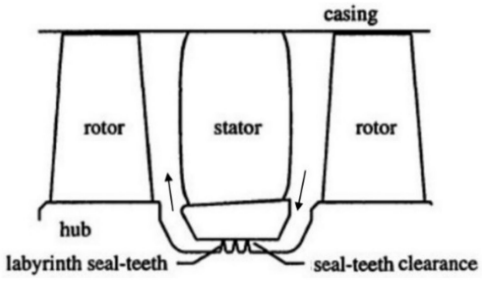

Figure 1. The seal cavity leakage in a compressor with shrouded stator.

Deterioration occurs during the operation of a jet engine and is reducing its performance continually. Reitz et al. [1] show that the change of blade tip gaps due to deterioration has a non-negligible influence on the compressor's performance. Wellborn et al. [2] showed that in a low-speed multistage compressor efficiency can be degraded by one point for every 1% increase in the seal-tooth clearance-to-span ratio. Considering the degradation is on the same scale as the penalty slope caused by rotor or stator tip clearances, it is reasonable to believe that the increase of the seal-tooth clearance due to deterioration during operation will have an important effect on the performance of the compressors.

Many studies have been conducted on the impact of seal cavity leakage flow on the compressor mainstream and the mechanism of the effect. Wellborn [2] presented data taken from a low-speed multistage axial flow compressor of which the labyrinth seal clearance was changed. A relation was developed from the measured data, that is, when the seal-tooth clearance-to-span ratio increases by 1%, the pressure rise decreases by 3%, and the efficiency decreases by one point. Therefore, Wellborn believes that the performance loss caused by leakage from the shrouded stator cavity is of the same order as that caused by tip clearance leakage. The same relation can also be found in the results measured by Ludwig [3]. In the experimental and numerical studies of two transonic rotors, Shabbir el al. [4] found that the seal cavity leakage flow would gather at the suction surface at the root of the blade, causing flow separation and performance degradation. In their research, the seal cavity leakage flow upstream of the rotor was modeled as inlet boundary conditions. LeJambre et al. [5] simulated an eleven-stage high pressure compressor and accounted for the effects of endwall flowpath cavities by the use of a simple 1D model. They demonstrated that an entrained seal cavity leakage flow leads to extra stator hub blockage developing in the power stream. The extra stator hub blockage results in the axial velocities increasing outboard of the 25% span, which further increases the negative incidence of the rear rotor, reduces the load and the total pressure rise of the blade row. An experimental study of leakage flow from shrouded stator cavity was completed by Wellborn and Okiish [6] in a low speed four stage compressor. In this work it was shown that the increasing seal cavity leakage not only worsens the flow field at the root of the stator row where the leakage flow occurs, but also changes the flow conditions at the stator exit over the entire span. As a result, in the following downstream stage, the work input of the rotor decreases and the total pressure loss of the stator increases, leading to a performance degradation at the next stage. Different from the experimental study of the whole four-stage compressor with multiple cavities, their numerical study was carried out on isentropic stator three and the corresponding cavity. Demargne and Longley [7] investigated the interactions between seal cavity leakage flow from the stator shroud and the main flow in a linear compressor cascade and suggested that besides the leakage flow rate, the cavity's tangential velocity is another key factor in the interaction process. The results clearly show that stator performance improves with the increase of the cavity's tangential velocity. Similar results can be found in reference [6,8,9]. Heidegger et al. [10] made an impressive 3D simulation investigating the influence of various shrouded stator cavity geometric parameters on an isolated stator row's performance.

In summary, seal cavity leakage flow through labyrinth seal-teeth exists in axial flow compressors with shrouded stator vanes. Although seal-tooth leakage has been shown to have a non-negligible impact on compressor performance, fewer simulations of the compressor together with the seal cavity leakage flow from the shrouded stator are available. In the literature mentioned above, the calculations of compressors with cavity leakage have been simplified to a certain extent. Either the effect of the cavity leakage flow is estimated by using a model, or the cavity is calculated simultaneously with only the isentropic stator. This general lack of simulation tools concerning seal cavity leakage flow from the shrouded stator makes it difficult to visually reflect the effect of seal cavity leakage flow in the design stage of compressor or in evaluating the performance degradation of compressors.

In order to provide a computational tool to quickly diagnose the influence of seal cavity leakage flow on compressor performance and internal flow field structure, the

circumferentially averaged dimensionality reduction method was used to do the coupling calculation of seal cavity leakage flow and single-stage compressor. As a kind of quasi three-dimensional simulation method, the circumferentially averaged method has its unique advantages. First of all, quasi-3D simulation can provide more abundant S_2 flow field information than 0D simulation. Secondly, quasi-3D simulation is easy to implement due to the small amount of calculation involved. Finally, for specific cases, the quasi-3D simulation can use an empirical model or semi-empirical model, such as a loss model or a blockage model obtained from the experimental data, to modify the flow field results so as to avoid the amplification of the flow field calculation error caused by the limitations of the turbulence model. These advantages make it easier to expand the research work on compressors to entire aeroengine simulations in the future.

In this paper, the main passage of a one stage compressor is numerically simulated together with the shrouded stator cavity by an inhouse circumferentially averaged method throughflow program (abbreviated as CAM) which can simulate axial compressors [11], centrifugal compressors, turbines and even combustion chambers [12]. Four configurations, which involved different seal-tooth leakage rates, were simulated. The effect of seal cavity leakage flow on the stator's performance and the interaction mechanism between the leakage flow and the main flow is investigated. The results indicate that the seal cavity leakage flow leads to an increased flow blockage near the hub, resulting in a drop of stator performance. The seal cavity leakage flow has a significant impact on the overall performance of the compressor, as well as a certain destructive effect on the flow field of the main passage and the performance of each blade row.

2. Throughflow Model and Research Object

The governing equations of CAM are dependent on the circumferentially averaged Navier-Stokes equations [11–13]. The equations are solved by a time-marching finite volume method. The JAMESON [14] scheme is adopted to discretize the inviscid fluxes. In order to discretize the viscous flux, the Green–Gauss theorem is applied to solve the gradient of the variable on the edge of a grid cell. As for the time discretization, an explicit Runge–Kutta 4 step method is put into use. In CAM, the Spalart–Allmaras (S–A) turbulence model was applied. Since the Mach number is below 0.3 in the shrouded cavity and above 0.3 in the main passage, preconditioning was applied to avoid the stiffness of compressible equation at low speed. At the same time, some measures to accelerate convergence were adopted, such as implicit residue averaging, local time step. The accuracy verification of the throughflow model by NASA Rotor 67 and a high-loaded transonic axial fan stage (ATS-2) can refer to reference [11]. The throughflow program has been applied to the first stage of a high-loading transonic six-stage compressor with inlet guide vane (IGV). The first stage with IGV has a design mass flow rate of 55.0 kg/s, a total to total pressure ratio of 1.81, and an adiabatic efficiency of 0.81. The flow path with sealing cavity is shown in Figure 2, where the geometric structure of the channel, cavity and labyrinth is simplified to some extent. The detailed geometric parameters of the flow path and blade are given in Tables 1 and 2 respectively.

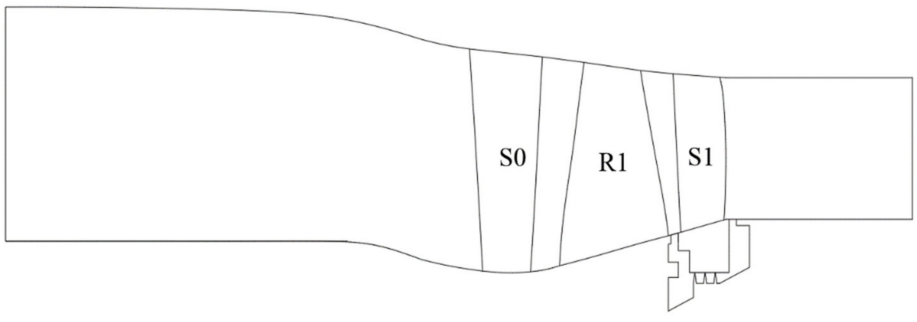

Figure 2. Flow path.

Table 1. The geometric parameters of flow path.

Parameters	Inlet	S0		R1		S1		Outlet
		Leading Edge	Trailing Edge	Leading Edge	Trailing Edge	Leading Edge	Trailing Edge	
hub radius/mm	198.76	173.40	172.94	177.94	203.43	206.41	216.93	217.44
shroud radius/mm	397.79	362.10	355.37	350.10	343.37	340.97	337.98	337.62

Table 2. The main blading parameters of the compressor.

Parameters	S0	R1	S1
No. of Airfoils	32	28	50
Chord/mm	51.65	103.26	46.27
Diameter/mm	724.20	700.20	681.95
Solidity	0.86	1.74	1.35
Aspect ratio	3.65	1.67	2.91
Inlet metal angle/(°)	0.47	−51.22	44.76
Outlet metal angle/(°)	8.16	−40.49	9.60

In Figure 3, the computational mesh is shown. The channel and the mainstream flow path grid are matched at the junction interface. To prove the reliability of the calculation results, it is necessary to verify the grid independence before the study. Sealing the labyrinth cavity is the key part of this study, so three kinds of cavity grids with different grid numbers were used to verify the grid independence. The topology of the mesh and the boundary conditions were set the same. The results are plotted in Figure 4. The curves of the case with 6975 cavity grid points coincide with that of the case with 15,357 cavity grid points, but they differ from the curves of the case with 4549 cavity grid points in adiabatic efficiency. In conclusion, when the number of grid points exceeds 6975, the results are considered independent of the grid number. In consideration of the calculation's accuracy and the requirement of saving time, the mesh with 6975 cavity grid points was used in this study.

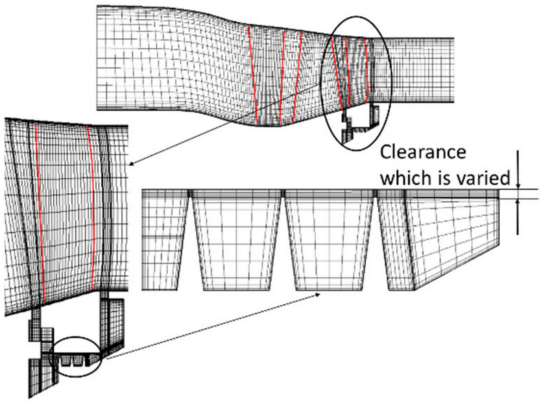

Figure 3. The computational mesh of the compressor with seal cavity leakage.

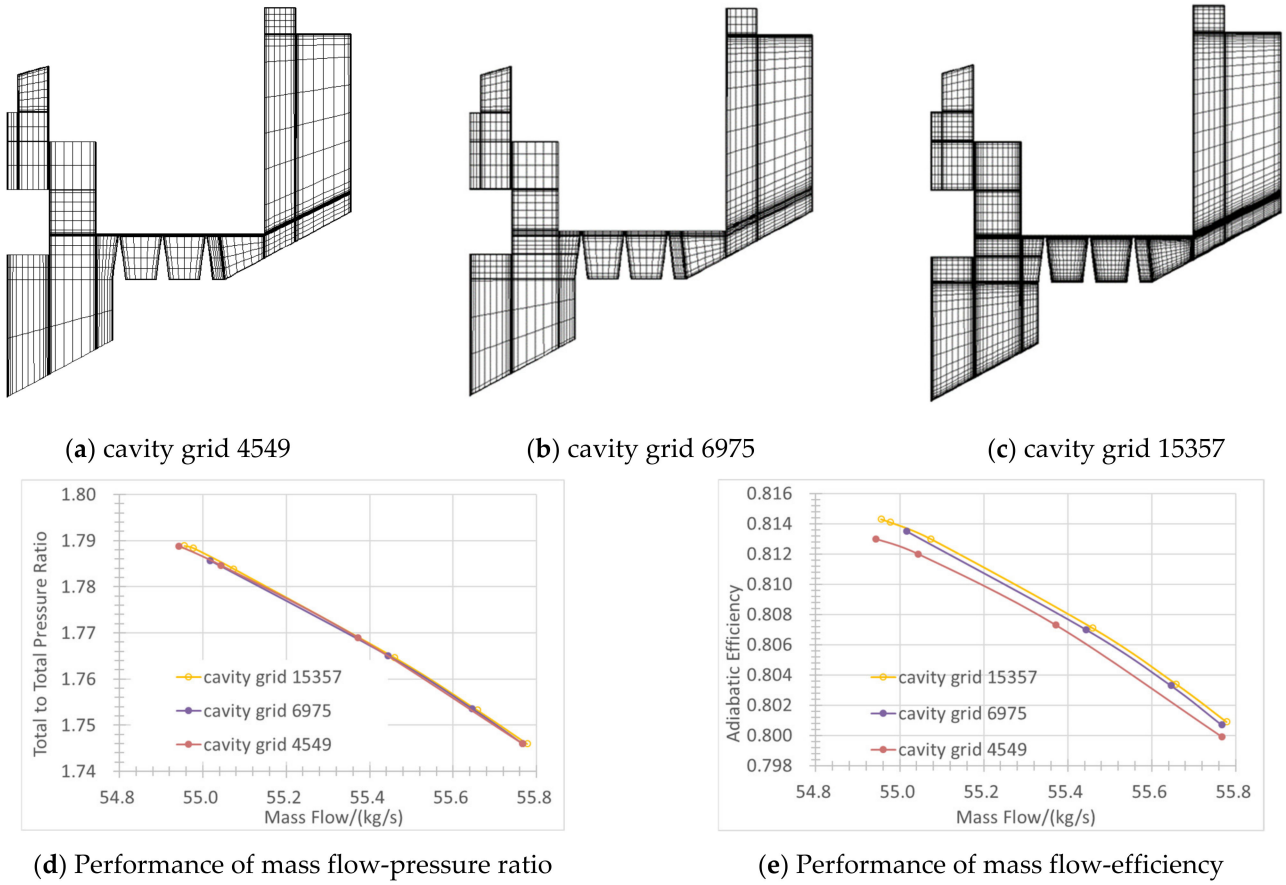

(**a**) cavity grid 4549 (**b**) cavity grid 6975 (**c**) cavity grid 15357

(**d**) Performance of mass flow-pressure ratio (**e**) Performance of mass flow-efficiency

Figure 4. Grid independence.

The boundary conditions are as follows: for the main flow of the compressor, the total temperature, total pressure and flow direction are given at the inlet, i.e., standard atmospheric conditions, horizontal intake. For different working conditions, given the corresponding static pressure at the outlet hub, the static pressure distribution along the spanwise direction at the outlet is obtained by using the simplified radial equilibrium equation. The numerical simulation is carried out at the design speed, i.e., 12,302 rpm.

Four configurations are set up to adjust the leakage flow by changing the size of the tip clearance (c) of the labyrinth. The setting of each configuration and the corresponding leakage flow rate (LF) calculated by CAM is shown in Table 3 (h is the blade height of S1). When c is 0, the seal cavity of the corresponding stage is removed, and only the mainstream flow path grid is retained.

Table 3. The clearance values and corresponding leakage flow rate for the different configurations.

Configuration	1	2	3	4
c/mm	0	0.5	0.75	1.0
c/h × 100	0	0.37	0.56	0.74
LF × 100	0	0.11	0.16	0.20

3. Results and Discussion

Figure 5a,b show the performance of the mass flow–total pressure ratio and the performance of the mass flow–adiabatic efficiency, respectively. It can be seen that when the leakage flow rate increases, both the total to total pressure ratio and efficiency of the compressor decrease significantly.

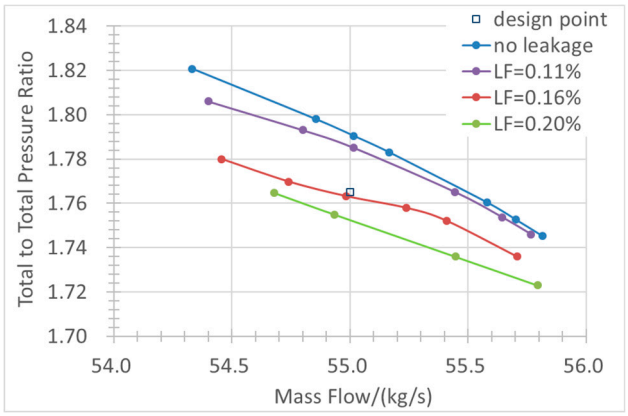

(**a**) Performance of mass flow-pressure ratio

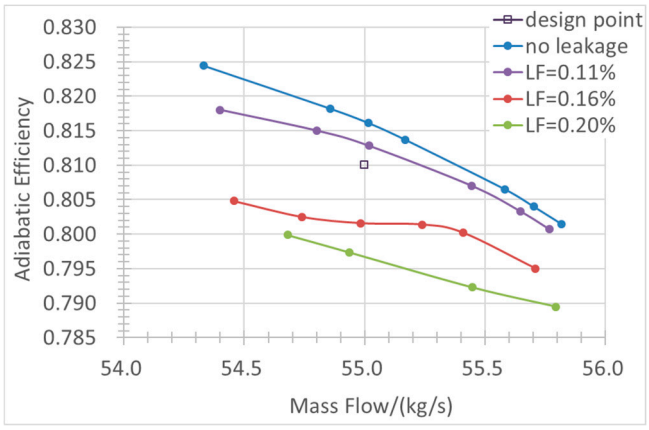

(**b**) Performance of mass flow-efficiency

Figure 5. The performance of the compressor.

A comparison of compressor performance parameters at the near design point (55 kg/s) is made between the case without or with seal cavity leakage flow, which is shown in Table 4. It can be seen that when compared with no leakage, the pressure ratio is reduced by 2% and the efficiency is reduced by 1.9% for a 0.74% increase of the seal-tooth clearance–to–span ratio.

Table 4. The comparison of compressor performance parameters at near design point.

	No Leakage	Clearance c = 0.5 mm	Clearance c = 0.75 mm	Clearance c = 1 mm
c/h × 100	0	0.37	0.56	0.74
LF = m_{LF}/m_{IN}	0	0.11%	0.16%	0.20%
Pressure ratio	1.7905	1.7850	1.7579	1.7549
Efficiency	0.8161	0.8128	0.8014	0.7974

The flow field comparison of the near design point with no leakage or 0.20% LF in the table is shown in Figures 6 and 7, which include the streamline traces and the absolute Mach number distribution. It can be seen from Figure 6 that the leakage flow enters the labyrinth structure of the cavity below the hub from the axial clearance behind the stator trailing edge, in which a vortex is formed many times. Then the leakage flow enters the mainstream from the axial clearance in front of the stator leading edge and mixes with it, forming a vortex at the stator root extending to the trailing edge of the stator. Due to the

existence of the whirlpool at the stator root, the mainstream migrates to the mid-span to a certain extent.

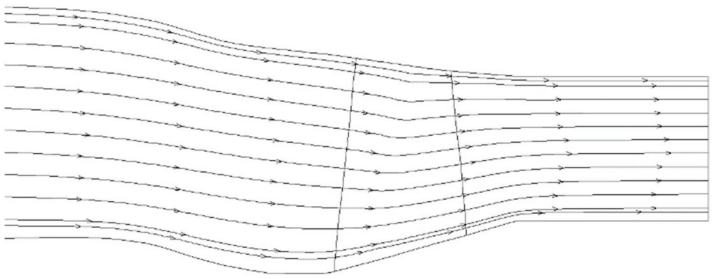

(**a**) No leakage

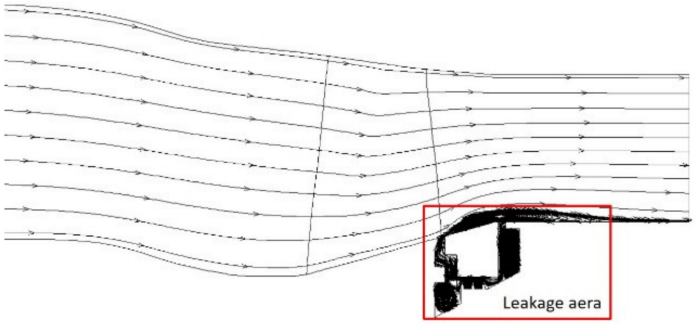

(**b**) Clearance c = 1 mm, LF = 0.20%

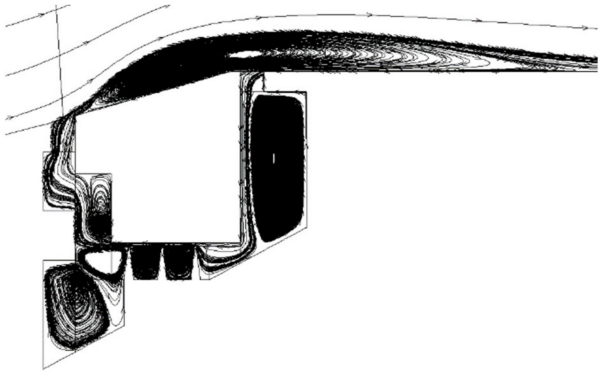

(**c**) Leakage aera

Figure 6. Streamline traces.

As shown in Figure 7, the flow velocity at the stator root is very low. Combined with the previous Figure 6, it can be seen that the mixing of the leakage flow and the mainstream reduces the flow capacity in the stator root passage and destroys the flow field structure.

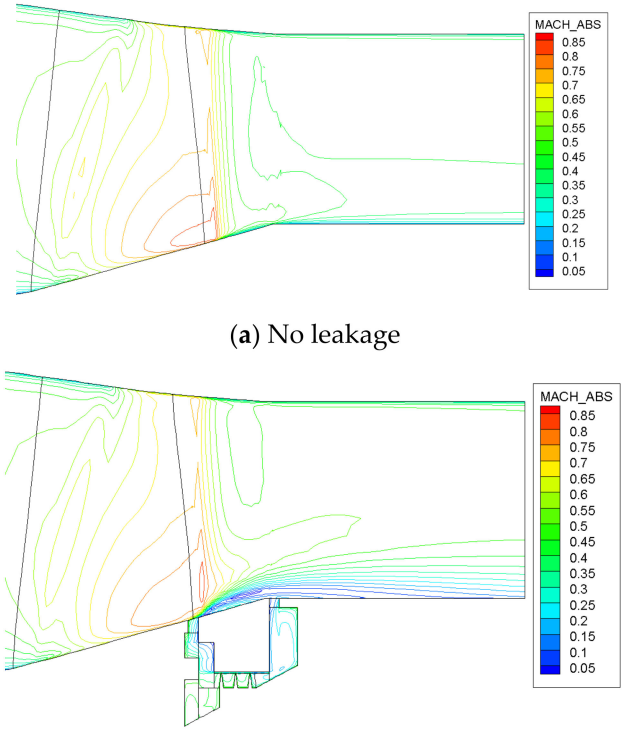

(**a**) No leakage

(**b**) Clearance c = 1 mm, LF = 0.20%

Figure 7. Absolute Mach number distribution.

The corresponding circumferentially averaged profiles of the total pressure recovery coefficient of the stator are illustrated in Figure 8. In Figure 8, the total pressure recovery factor of the stator without leakage flow has a depression in the 7% elevation range near the root. The increase in leakage flow further enlarges the depression. As the leakage flow rate increases from 0.11% to 0.20%, the penalty of the total pressure recovery coefficient of stator root increases from 0.1 to 0.2, and the depression increases from 10% to nearly 30% in the spanwise direction, indicating that the seal cavity leakage flow has a certain destructive impact on the performance of the stator. The reasons may be as follows: on the one hand, the total pressure loss occurs when part of the fluid flows from the stator exit to the stator inlet through the cavity and the labyrinth seal under the hub, which makes the total pressure loss at the stator root higher relative to that without leakage flow; on the other hand, since the mixing of the low-energy inlet leakage with the mainstream at the leading edge of the stator, incidence changes as well as the axial momentum decreases (reflecting flow blockage), which in turn destroys the flow structure at the stator root and further increases its loss. It should be noticed that the decrease in axal momentum reflects the blockage of flow. The third point is that the incident leakage flow at the leading edge of the stator has a certain radial velocity, which together with the flow blockage induces spanwise migration, thus increasing the total pressure recovery coefficient at the middle of the stator and decreasing the total pressure recovery coefficient at the root of the stator, which is also reflected in Figure 6.

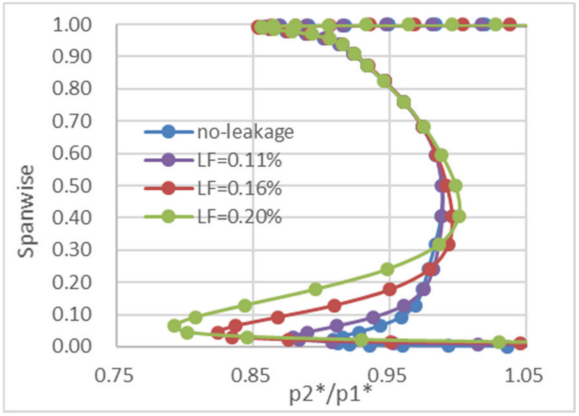

Figure 8. The radial distribution of the Stator's total pressure recovery coefficient.

It was previously suggested that the seal cavity leakage flow in the clearance may increase the loss at the root of the stator by changing the incidence and destroying the structure of the flow field, thus further affecting the pressure ratio and efficiency of the single stage compressor. Figures 9 and 10 confirm this hypothesis. Figure 9 is a sketch map of the spanwise distribution of the stator inlet incidence. It can be seen that with the increase in leakage flow rate, the incidence at the stator root (below 10% elevation) increases dramatically. This will lead to flow separation and further blockage of the blade passage, which in turn reduces the total pressure recovery coefficient. The high incidence characteristic of the stator root reflects that the flow capacity of the fluid in the root is weak and the axial momentum is small. However, with the increase in leakage flow rate, the overall decrease of the incidence above 20% elevation indicates that the leakage flow induces the flow to migrate toward the blade tip. Considering the fact that the amount of leakage flow is very small (no more than 0.20% of the mainstream), the spanwise migration is mainly caused by the blockage of the stator root flow induced by the leakage flow rather than the radial velocity of the leakage flow itself.

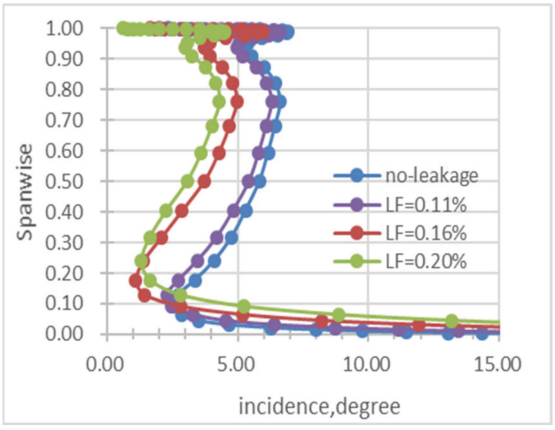

Figure 9. The radial distribution of the Stator's inlet incidence.

Figure 10a,b show the distribution of fluid axial momentum divided by a unified reference value along the spanwise direction at the leading edge of the stator (downstream the left branch of the cavity) and at the 1.5 chord length downstream of the trailing edge of stator (downstream of the right branch of the cavity). As can be seen both from Figure 10a,b, the influence of leakage flow on the stator flow field is not limited to the hub region, but extends to the whole span. The axial momentum of the fluid decreases gradually with the increase of leakage flow at the stator root near the hub (below 10% span). The decrease in axial momentum reflects the increase in flow blockage. The flow blockage at the stator root causes the spanwise migration

of the flow, and the axial momentum in the middle span of the blade increases accordingly. The variation of inlet axial momentum to leakage flow in Figure 10a is consistent with that of incidence to leakage flow in Figure 9.

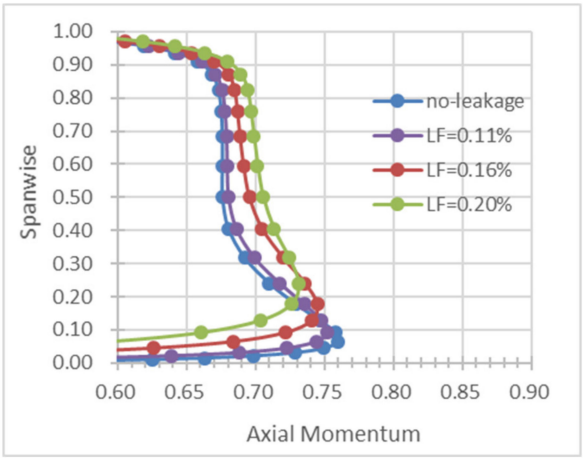

(**a**) stator inlet

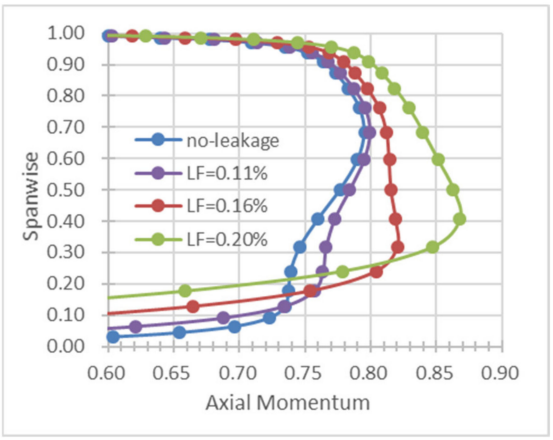

(**b**) 1.5 times chord strength downstream of stator outlet

Figure 10. The radial distribution of axial momentum.

In order to further verify the previous analysis, the corresponding spanwise static pressure ratio distribution of the stator was compared, as shown in Figure 11. As the leakage flow increases, the static pressure ratio of stator decreases in the whole span, and the reduction at the hub area is greater. This is consistent with the previous analysis. For a specific working condition, the spanwise position of the maximum static pressure rise increases with the increase in leakage flow rate, which reflects the spanwise migration caused by leakage flow.

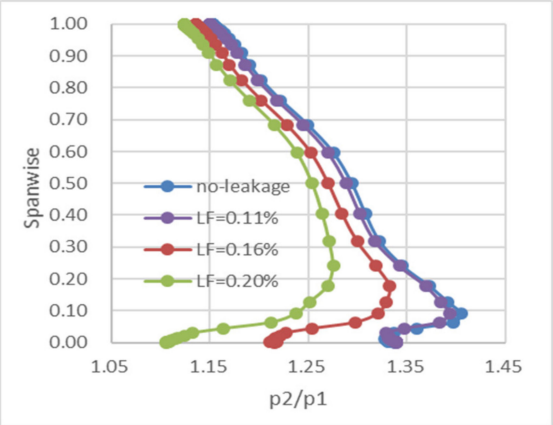

Figure 11. The radial distribution of the Stator's static pressure ratio.

4. Conclusions

Results from numerical simulations indicate that seal cavity leakage flow though the cavity and the labyrinth seal under a shrouded stator of moderate hub/tip ratio can have a significant and detrimental impact on the performance of a compressor. Compared with no leakage, the pressure ratio can be reduced by 2% and the efficiency can be reduced by 1.9% for a 0.74% increase of seal-tooth clearance-to-span ratio. The major findings of this study can be summarized as follows:

(1) With the increase in leakage flow rate, both the total to total pressure ratio and the efficiency of the compressor decrease significantly.
(2) With the leakage flow rate increasing, the incidence at the stator root increases dramatically, which reflects the hub blockage caused by seal cavity leakage, and the incidence above 20% spanwise decreases overall, which reflects the spanwise migration induced by hub blockage.
(3) The axial momentum of the fluid decreases gradually with the increase in leakage flow at the stator root near the hub, which reflects the hub blockage caused by seal cavity leakage. The reduction in axial momentum at the hub with leakage addition causes an increase in axial momentum higher up the span, which reflects the spanwise migration induced by the hub blockage.
(4) The increase in hub incidence and hub blockage as well as spanwise migration induced by seal cavity leakage in turn reduces the effective flow area, thus reducing the diffusion within the stator passage. The result is a reduction in pressure ratio as well as efficiency.
(5) Compared with the traditional design, which only considers the mainstream in compressors, the design incidence at the root of the shrouded stator should be increased and the design incidence at middle span should be reduced in order to make the stator blade more suitable for the changed flow field under the impact of seal cavity leakage flow.

Overall, the circumferentially averaged throughflow model can reasonably reflect the influence of leakage flow on the performance and flow field of a single-stage axial compressor. This study provides a diagnostic tool to quickly analyze the effect of seal cavity leakage flow during compressor design and performance degradation, which lays a solid foundation for further research on the influence of leakage flow in multistage compressors.

Author Contributions: Conceptualization, D.L. and X.G.; methodology, D.L.; software, D.L.; validation, D.L.; formal analysis, D.L.; investigation, D.L.; resources, D.L.; data curation, D.L.; writing—original draft preparation, D.L.; writing—review and editing, D.L., D.J. and X.G.; project administration, D.J. All authors have read and agreed to the published version of the manuscript.

Funding: This research was funded by the National Science and Technology Major Project (2017-I-0005-0006).

Institutional Review Board Statement: Not applicable.

Informed Consent Statement: Not applicable.

Data Availability Statement: Data sharing is not applicable to this article.

Acknowledgments: The authors would like to thank Fang-fei Ning for the guidance and kind advice, and the fellow apprentices in the research group for their help.

Conflicts of Interest: The authors declare no conflict of interest.

Abbreviations

Nomenclature

c	labyrinth clearance
p	static pressure
p^*	total pressure
m	massflow rate
LF	leakage flow rate
h	blade height of S1

Subscripts

IN	the inlet of compressor
LF	seal cavity leakage flow

References

1. Reitz, G.; Kellersmann, A.; Friedrichs, J. Full High Pressure Compressor Investigations to Determine Aerodynamic Changes due to Deterioration. In Proceedings of the ASME Turbo Expo 2018: Turbomachinery Technical Conference and Exposition, Oslo, Norway, 11–15 June 2018; ASME: New York, NY, USA, 2018.
2. Wellborn, S.R. Effects of Shrouded Stator Cavity Flows on Multistage Axial Compressor Aerodynamic Performance. Ph.D. Thesis, Iowa State University, Ames, IA, USA, 1996.
3. Ludwig, L.P.; Bill, R.C. Gas Path Sealing in Turbine Engines. *J. ASLE Trans.* **1980**, *23*, 1–22. [CrossRef]
4. Shabbir, A.; Celestina, M.L.; Adamczyk, J.J.; Strazisar, A.J. The Effect of Hub Leakage Flow on Two High Speed Axial Flow Compressor Rotors. In Proceedings of the International Gas Turbine and Aeroengine Congress and Exhibition, Orlando, FL, USA, 2–5 June 1997; ASME: New York, NY, USA, 1997.
5. LeJambre, C.R.; Zacharias, R.M.; Biederman, B.P.; Gleixner, A.J.; Yetka, C.J. Development and Application of a Multistage Navier-Stokes Flow Solver: Part II—Application to a High Pressure Compressor Design. In Proceedings of the International Gas Turbine and Aeroengine Congress and Exposition, Houston, TX, USA, 5–8 June 1995; ASME: New York, NY, USA, 1995.
6. Wellborn, S.R.; Okiishi, T.H. The influence of shrouded stator cavity flows on multistage compressor performance. In Proceedings of the International Gas Turbine and Aeroengine Congress and Exhibition, Stockholm, Sweden, 2–5 June 1998; ASME: New York, NY, USA, 1998.
7. Demargne, A.A.J.; Longley, J.P. The Aerodynamic Interaction of Stator Shroud Leakage and Mainstream Flows in Compressors. In Proceedings of the ASME Turbo Expo 2000: Power for Land, Sea, and Air, Munich, Germany, 8–11 May 2000; ASME: New York, NY, USA, 2000.
8. Wellborn, S.R.; Tochinsky, I.; Okiishi, T.H. Modeling shrouded stator cavity flows in axial-flow compressors. In Proceedings of the International Gas Turbine and Aeroengine Congress and Exhibition, Indianapolis, IN, USA, 7–10 June 1999; ASME: New York, NY, USA, 1999.
9. Wellborn, S.R. Details of Axial-Compressor Shrouded Stator Cavity Flows. In Proceedings of the ASME Turbo Expo 2001: Power for Land, Sea, and Air, New Orleans, LA, USA, 4–7 June 2001; ASME: New York, NY, USA, 2001.
10. Heidegger, N.J.; Hall, E.J.; Delaney, R.A. Parameterized Study of High-Speed Compressor Seal Cavity Flow. In Proceedings of the AIAA, ASME. SAE, and ASEE, 32nd Joint Propulsion Conference and Exhibit, Lake Buena Vista, FL, USA, 1–3 July 1996. AIAA Paper 96-2807.
11. Jin, H.L.; Jin, D.H.; Li, X.J.; Gui, X.M. A Time-Marching Throughflow Model and its Application in Transonic Axial Compressor. *J. Therm. Sci.* **2010**, *19*, 519–525. [CrossRef]
12. Wan, K.; Tang, M.Z.; Jin, D.H.; Gui, X.M. Analysis of Circumferential Fluctuation in Compressor Cascades. In Proceedings of the ASME Turbo Expo 2014: Turbine Technical Conference and Exposition, Düsseldorf, Germany, 16–20 June 2014; ASME: New York, NY, USA, 2014.

13. Liu, X.H.; Jin, D.H.; Gui, X.M. Throughflow Method for a Combustion Chamber with Effusion Cooling Modelling. In Proceedings of the ASME Turbo Expo 2018: Turbomachinery Technical Conference and Exposition, Oslo, Norway, 11–15 June 2018; ASME: New York, NY, USA, 2018.
14. Jameson, A.J.; Schmidt, W.; Turkel, E. Numerical Solution of the Euler Equations by Finite Volume Methods Using Runge-Kutta Time Stepping Schemes. *Aiaa Journal* **1981**, 1259.